AVAILABLE AT
www.ElsevierComputerScience.com
POWERED BY SCIENCE DIRECT®

PERGAMON

Neural Networks 16 (2003) 1141–1160

Neural Networks

www.elsevier.com/locate/neunet

A neural network simulating human reach–grasp coordination by continuous updating of vector positioning commands

Antonio Ulloa*, Daniel Bullock

Department of Cognitive and Neural Systems, Boston University, 677 Beacon Street, Boston, MA 02215, USA

Received 4 November 2002; revised 25 March 2003; accepted 25 March 2003

Abstract

We developed a neural network model to simulate temporal coordination of human reaching and grasping under variable initial grip apertures and perturbations of object size and object location/orientation. The proposed model computes reach–grasp trajectories by continuously updating vector positioning commands. The model hypotheses are (1) hand/wrist transport, grip aperture, and hand orientation control modules are coupled by a gating signal that fosters synchronous completion of the three sub-goals. (2) Coupling from transport and orientation velocities to aperture control causes maximum grip apertures that scale with these velocities and exceed object size. (3) Part of the aperture trajectory is attributable to an aperture-reducing passive biomechanical effect that is stronger for larger apertures. (4) Discrepancies between internal representations of targets partially inhibit the gating signal, leading to movement time increases that compensate for perturbations. Simulations of the model replicate key features of human reach–grasp kinematics observed under three experimental protocols. Our results indicate that no precomputation of component movement times is necessary for online temporal coordination of the components of reaching and grasping.

Keywords: Neural network; Reaching and grasping; Human prehension; Precision grip; Reach–grasp coordination; Vector-integration-to-endpoint

1. Introduction

Reaching for and grasping a static object involves the coordination of three components: hand/wrist transport, grip aperture, and hand orientation. The 'transport component' consists of a single phase that involves the movement of the hand/wrist from an initial position to a final position that is close to the object being reached. The 'aperture component' consists of two sequential phases. 'Preshaping' opens the grip, slowly and monotonically, to a maximum aperture, and 'enclosing' reduces the aperture quickly until the fingers contact the object. The third component, 'hand orientation', quantifies changes, in alignment of the hand axes, that make it convenient for the hand to grasp the object.

The main kinematic features of prehension movements have been identified in previous studies of transport and aperture formation. As shown in Fig. 1, there is a parallel evolution of hand/wrist transport and grip aperture, and both of them start and end approximately simultaneously (Jeannerod, 1984). The transport phase exhibits a unimodal, relatively symmetrical tangential velocity profile of the hand/wrist (Atkeson & Hollerbach, 1985; Morasso, 1981). The grip aperture shows an opening to a maximum aperture greater than the object size followed by closing upon the object (Jakobson & Goodale, 1991; Jeannerod, 1984; Wallace & Weeks, 1988).

The present paper presents a neural network model that simulates timing coordination in reaching to grasp static objects, and that naturally adapts to open initial hand apertures, perturbations of object size, and perturbations of object location/orientation.

2. Background

2.1. Data constraints

The following summary is based solely on experiments on human prehension. However, recent data (Roy, Paulignan, Farne, Jouffrais, & Boussaoud, 2000) show that

* Corresponding author. Present address: National Institutes of Health, 9000 Rockville Pike, Building 10, Room 3C716, Bethesda, MD 20892, USA. Tel.: +1-301-435-5141; fax: +1-301-480-5625.
E-mail address: antonio.ulloa@nih.gov (A. Ulloa).

0893-6080/03/$ - see front matter © 2003 Elsevier Ltd. All rights reserved.
doi:10.1016/S0893-6080(03)00079-0

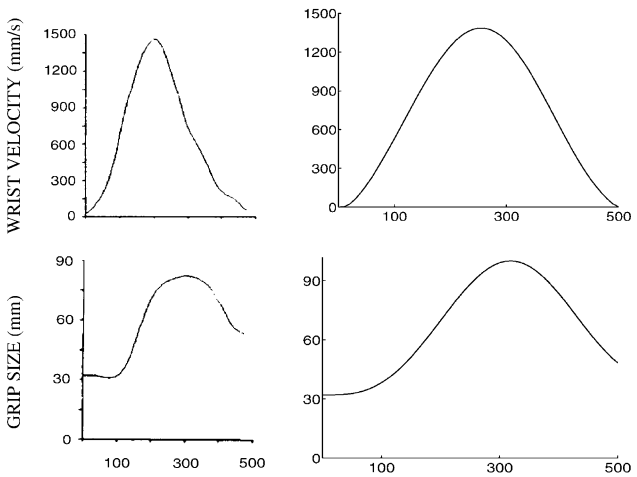

Fig. 1. Wrist velocity and grip aperture (size) for a basic prehension movement (left column) and simulation of that movement (right column). After opening to a size greater than the objects, the grip closes to a final aperture equal to object size. Transport distance was set to 36 cm, object size was 1.5 cm. GO amplitude was set to 45. The simulated hand aperture plot was shifted by 3.2 cm to match the shift in position included in the data plot. This shift reflects the offset between the grasping surface of the fingers and the position of the recording markers on the fingers of experimental subjects. The data plots were reproduced with permission from Paulignan et al. (1991b, Fig. 2, p. 505), Copyright ©1991 Springer-Verlag.

many of the principles also apply to prehension in other primates.

2.2. Maximum grip aperture timing

Maximum grip aperture occurs at about 60–80% of movement time. Wallace and Weeks (1988) instructed subjects to grasp a small object (3 mm) at different distances (30 and 15 cm) and within a specified movement time (200 and 400 ms). Subjects were told to grasp the target object with a pinch grip as accurately as possible. Results of this experiment showed occurrences of maximum grip apertures between 61 and 67.8% of movement time. Similarly, Jeannerod (1984) found a small band of relative times of occurrence of maximum aperture (74–81%) by using object widths between 2 and 8 cm, at distances of 25, 32, and 40 cm. Further, Paulignan and Jeannerod (1996) reported maximum aperture occurrence at 70–80% of movement time, and Jakobson and Goodale (1991) noted the peak aperture to occur right after two-thirds of movement time. Thus, the grip aperture of a reach–grasp movement invariably peaks at about 60–80% of movement time.

2.3. Factors that affect grip aperture size

Faster reach–grasp movements lead to larger maximum grip apertures. Wing, Turton, and Fraser (1986) instructed subjects to grasp objects at two speeds, normal and fast. The normal speed was chosen by the subject and the fast one was ‘as fast as possible’ without dropping the object. The size of the object was 2.8 cm and it was located at 28 cm from the hand’s initial position. The mean movement times obtained in this task were 376 ms for the fast movement, and 735 ms for the normal movement. Larger maximum apertures were observed for the faster movements. Thus, faster reach–grasp movements lead to larger maximum grip apertures.

Reach–grasp movements that start with an open grip aperture show a tendency of the hand grip to partially close before achieving its maximum aperture. Saling, Mescheriakov, Molokanova, Stelmach, and Berger (1996) experimented with two types of grasping, normal and ‘altered’. A normal grasp initiated with the fingers relaxed, whereas an altered grasp initiated with the fingers maximally extended. Representative trials of those experiments are shown in the left side of Fig. 2, which depicts, for the altered case, an initial aperture reduction phase followed, sometimes after a pause (zero value of the velocity trace), by a small reopening of the grip aperture, and the final enclosing phase. In addition, the enclosing phase appeared to begin at or just before the time typical for normal prehension. In the same way, Timmann, Stelmach, and Bloedel (1996) instructed subjects to reach a small (0.7 cm) object at 28 cm, starting with the hand fully extended; they observed that the hand closed in the first part of the movement, to reopen and close again. Thus the hand grip during a reach–grasp movement has a natural tendency to close, and this effect is especially observed when a reach–grasp movement starts with an open grip aperture.

2.4. On-line movement corrections

Object location perturbations cause the reach–grasp movement to pause to allow for corrections of movement. Paulignan, MacKenzie, Marteniuk, and Jeannerod (1991b) investigated the effects of perturbations to object location on the coordination between transport and aperture control. In these experiments, the position of the object was unexpectedly shifted at movement onset. Two transparent objects were used (1.5 cm in diameter), so that the illumination could be switched from one object to the other. The objects were located at either 20 and 10° or 20 and 30° with respect to the body midline. The left side of Fig. 3 shows a trial for an unperturbed case and a trial for a perturbed case (20–30°). Both components, transport and aperture, were affected by the perturbation. Movement time was longer in the perturbed case and this allowed time for corrections in movement. Paulignan et al. reported a 250–290 ms delay before complete correction of the wrist trajectory and a lengthening by 100 ms of movement time (on average). Thus, perturbations of the target object location of a reach–grasp movement cause a pause in the movement as a whole in order to accommodate the movement to the new target location.

Object size perturbations at movement onset cause the reach–grasp movement to pause to allow for corrections of movement. Paulignan, Jeannerod, MacKenzie, and Marteniuk (1991a) conducted experiments with small

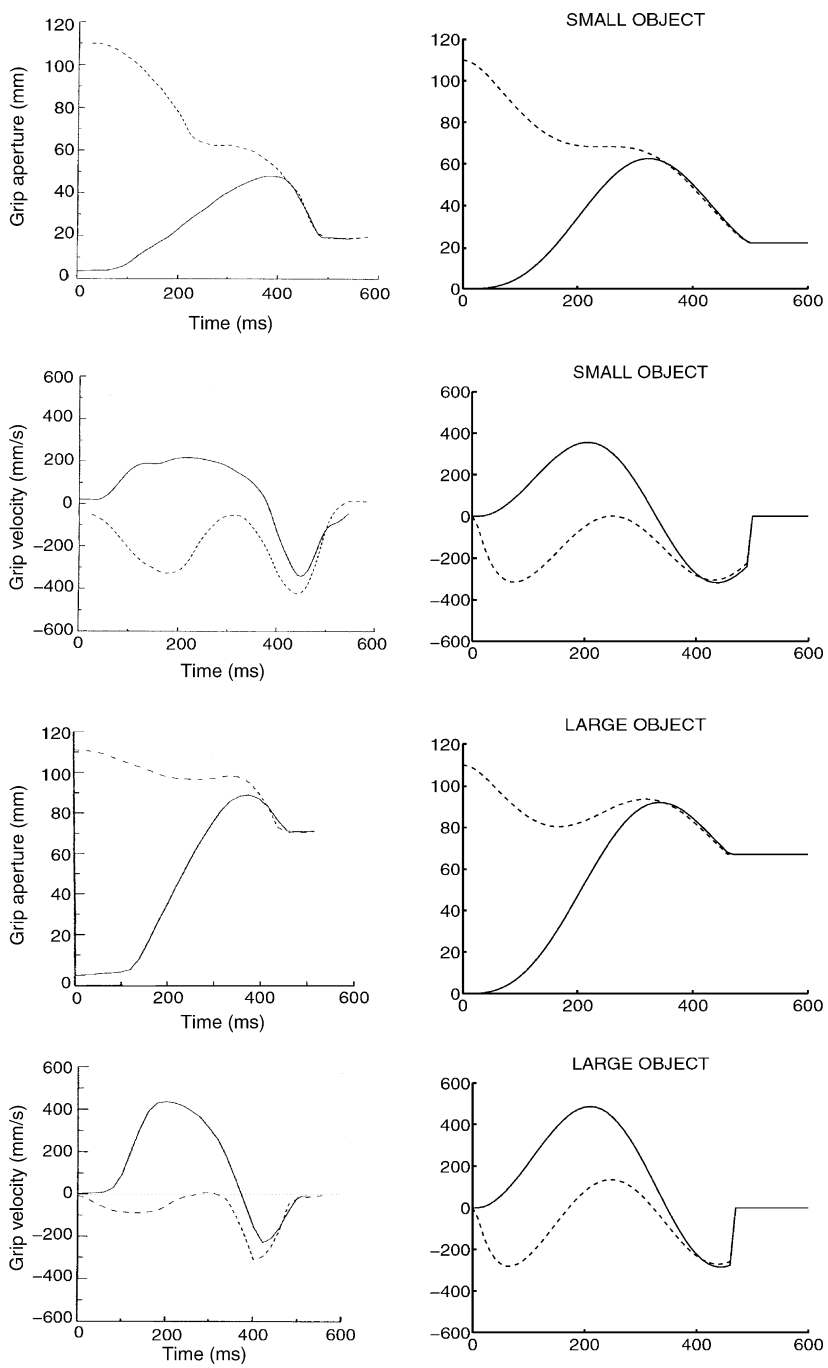

Fig. 2. Data (left column) and simulations (right column) showing aperture kinematics with normal and initially open grip apertures. Continuous lines represent normal grasping movements begun with the hand closed. Dashed lines represent movements with an initially fully open grip aperture. Object sizes were 2.2 and 6.7 cm. The object was located at 30 cm from the subject. Data reproduced with permission from Saling et al. (1996, Figs. 1 and 2, p. 495). Copyright ©1996 Springer-Verlag.

(1.5 cm) and large (6 cm) objects that were located 35 cm away from the subject. The objects were transparent, so that either the small or the large one was illuminated. The perturbations of object size were introduced at movement onset. The left side of Fig. 4 shows the effects of small-to-large (S–L) and large-to-small (L–S) perturbations on the grasping kinematics. In the S–L perturbation, the grip aperture first increases to the peak corresponding to the small object, and increases again to a maximum aperture corresponding to the large object, to finally close around the object. Thus, perturbations of the size of the target object (at movement onset) of a reach–grasp movement cause a pause in the movement as a whole in order to accommodate the movement to the new target size.

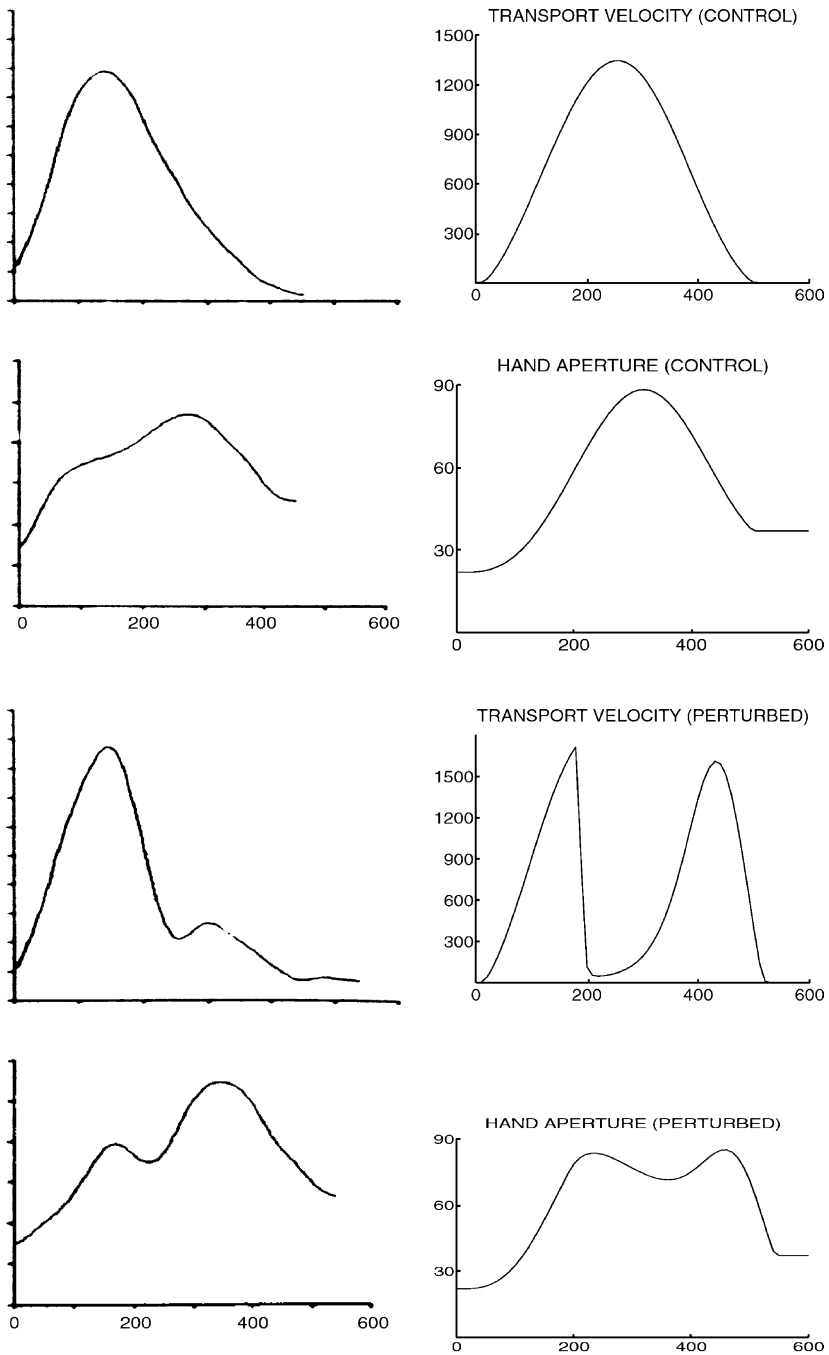

Fig. 3. Data (left column) and simulations (right column) showing transport and aperture kinematics when a 1.5 cm cylindrical object's location was unexpectedly shifted from 20 to 30° with respect to body midline. The upper two rows of plots illustrate tangential wrist velocity (row one) and grip aperture (row two) for an unperturbed grasp. The lower two rows of plots illustrate tangential wrist velocity (row three) and grip aperture (row four) for a perturbed grasp. Data reproduced with permission from Paulignan et al. (1991b, Fig. 6, p. 508). Copyright ©1991 Springer-Verlag.

2.5. Prior models

2.5.1. The Hoff–Arbib model

A model for reaching and grasping was proposed by Hoff and Arbib (1993). In this model, estimated times for transport and opening are applied to coordinate transport with aperture control. Fig. 5 shows the main features of this model, which has a stage that estimates movement time before the movement starts. This estimation of movement time works in the following manner. First, reaching distance and object size are estimated, based on visual information. Next, reaching distance and object size are used to estimate movement time for transport, and object size is used to estimate opening time. Then, enclose time, which is assumed constant for a particular task, is added to opening time, to form a second estimated movement time. Finally, the maximum of the two estimates is used as the actual movement time for transport. To compute opening time,

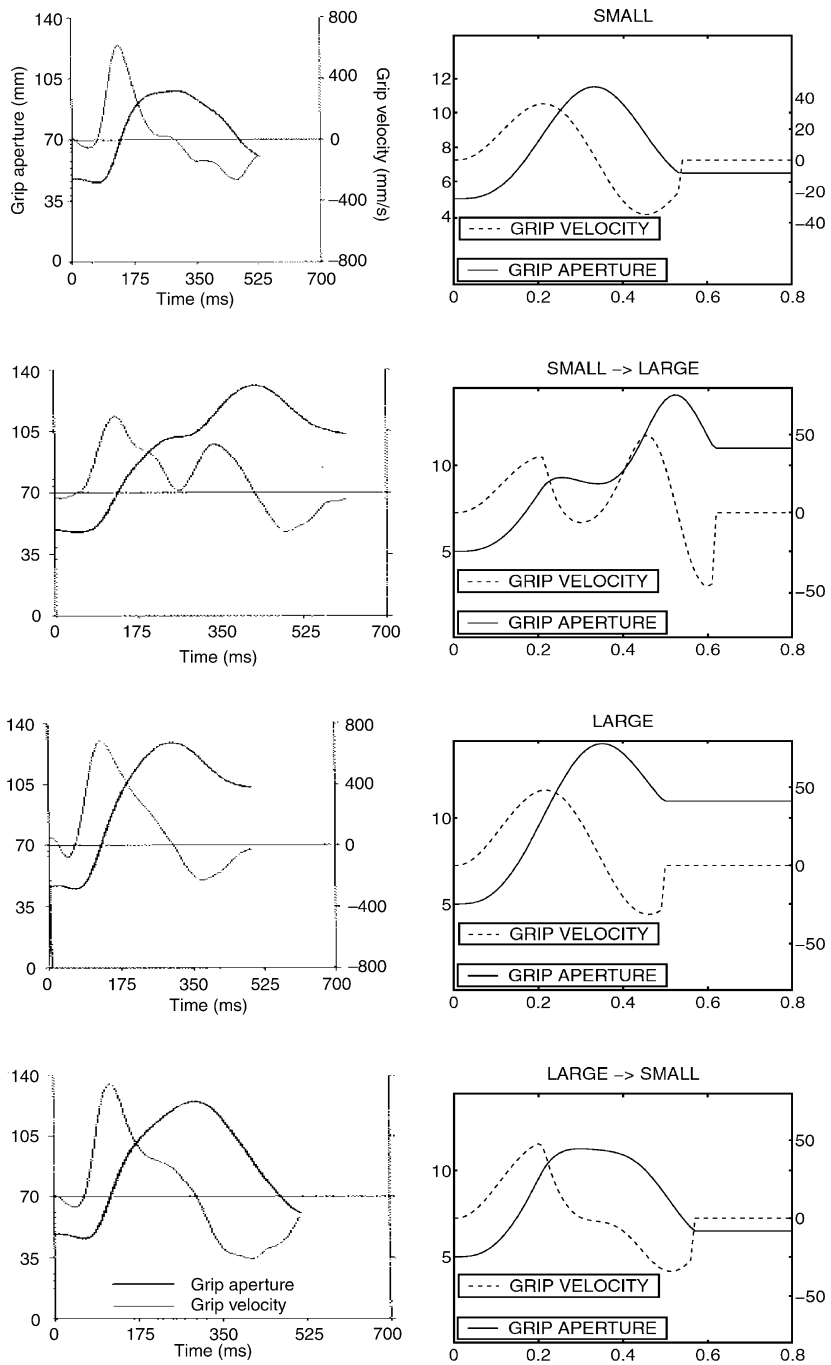

Fig. 4. Data (left column) and simulations (right column) showing grip aperture kinematics when object size was unexpectedly increased or decreased at the onset of movement. Two cylindrical objects were used, of 1.5 and 6 cm in diameter. In a perturbed trial, the object was shifted from small to large, or vice versa. From top, row one shows a grasping movement for an unperturbed trial, small object; row two shows a perturbed trial, in which the object was shifted from small to large. Row three shows a grasping movement for an unperturbed trial, large object; and row four shows a perturbed trial, in which the object was shifted from large to small. Data reproduced with permission from Paulignan et al. (1991a, Fig. 8, p. 416). Copyright ©1991 Springer-Verlag.

the enclose time is then subtracted from movement time. Thus the model effectively adjusts the component times to accommodate the fixed enclose time.

After the premovement stage, the transport and opening controllers are activated concurrently; when the opening controller achieves its goal, it triggers the activation of an enclose controller. The transport controller is a feedback controller based on minimum-jerk optimization criteria, with a cost function that penalizes inaccuracy, variability, and lack of smoothness in the movement trajectory. This controller takes as input the time remaining for movement, r, which is computed as the difference between final and current times, $t_f - t_c$. This controller also keeps track of the hand state $s = [p, v, a]$, where p, v, and a are position, velocity and acceleration of the hand, respectively. If the current hand state is perturbed, say from s to s_p, then

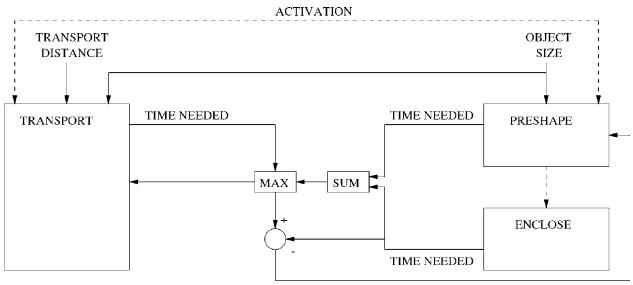

Fig. 5. The Hoff–Arbib model for prehension. Adapted from Hoff and Arbib (1993).

the system generates another trajectory from s_p to the final state s_f, within the time remaining from the moment of the perturbation. The controllers for opening and enclose are feedback controllers with an optimization criterion that assigns costs to hand opening and closing acceleration. Whereas the opening controller generates a trajectory from initial aperture to maximum aperture, the enclose controller generates a trajectory from maximum aperture to object size.

The target of the opening controller is maximum aperture, which is estimated as three-fourths of object size plus 4.55 cm. Although this relationship was observed to hold for several sizes, it cannot fit the data in Wallace and Weeks (1988) for the case of a 3 mm object size. For this size, this estimation predicts a maximum aperture of 4.78 cm, whereas the empirical maximum aperture reported by Wallace and Weeks (1988) was on the order of 9.5–11.2 cm. Thus, this estimation of maximum aperture, implemented as a linear mapping from object size to maximum aperture, fails to predict some of the data. The reason for this failure is that this estimation does not consider transport velocity, which contributes to grip opening (Wing et al., 1986).

The enclose controller uses a pre-set remaining time. Although enclose time was hypothesized to be constant across perturbations for a particular task, Zaal, Bootsma, and van Wieringen (1998) have since found that enclose time increases with the amplitude of transport. Also, Hofsten and Ronnqvist (1988) reported an inverse relation between enclose time and object size.

The Hoff and Arbib (1993) model uses two independent feedback controllers to generate two separate trajectories for transport and aperture. This is compatible with the so-called visuomotor channels hypothesis (Jeannerod, 1984, 1989; Paulignan & Jeannerod, 1996). According to this view, there are independent controllers for transport and aperture, and none of the controllers have information about how the other controller is progressing during movement execution. Consequently, these controllers do not share either spatial or temporal state information. In this theory, errors due to perturbations would only cause corrections in the specific channel in which such a perturbation occurred, unless an external perturbation directly affects more than one channel, as in the case where a change in object size affects both required hand aperture and required movement distance, or the case where a change in object position restarts the entire grasping process. Likewise, the Hoff–Arbib model postulates that transport and aperture are only synchronized in time to enable both processes to finish at the same time. For this reason, this model falls into the class of models that use separate independent channels for execution, with only an initial time synchronization.

A useful aspect of the Hoff–Arbib model is the use of different controllers for each of the three components of prehension, working in parallel. The evidence seems to show that these are processes that can be distinguished from each other, although not at the level of only linking them through time constraints.

There are two alternative views to the independent channels hypothesis: the Zaal et al. (1998) view and the Haggard and Wing (1995) view. Based on their discovery that enclose time increases with transport amplitude, Zaal et al. (1998) proposed that there is a dynamical coupling in both directions between transport and aperture, and that this coupling is based on time-to-contact information. Zaal et al. presented a model of the coupling from the transport component to the aperture component of prehension. In this model, the reaching action of the hand towards the object generates the information that is used to coordinate the aperture component. This is a dynamical model in which open and closed grip apertures are defined as attractors in a dynamical system (or wells in a potential field). An open grip position is represented by an attractor located at -1, whereas a closed grip position is represented by an attractor located at $+1$. The shape, width and depth of the two attractors are determined by corresponding constants within the system. The aperture dynamics are coupled to visual information specifying time-to-contact with the object. During evolution of grip aperture, the attractor for the open grip aperture state decreases its attraction, whereas the attractor for the closed grip aperture state increases its attraction. This effect is achieved through the influence of time-to-contact information on aperture dynamics. Although the simulations of this model provided a good fit for enclose phase onset timing for static and moving objects, it is not capable of simulating spatial trajectories for hand/wrist transport and grip aperture.

Because the present model shares more in common with Haggard and Wing's model than with Zaal et al.'s, Haggard and Wing's will be treated in detail in Section 2.5.2.

2.5.2. The Haggard–Wing model

Haggard and Wing (1995) proposed a model for coordination of reaching and grasping. In this model, both processes, transport and aperture control, have access to each other's spatial state. In a reach–grasp experiment, Haggard and Wing found, after a pull perturbation to the arm, that the fingers exhibited a tendency to return to a closed position. They analyzed the spatial relation between transport and aperture and noted a stereotyped underlying

spatial relation between the two components. This spatial relation consisted of a slow increment of hand aperture during most of arm transport development, and a fast hand closing in the last centimeters of arm transport. When perturbations occurred, the aperture exhibited a tendency to return to this spatial relation. Based on these findings, Haggard and Wing proposed that the shaping of the hand is intimately dependent on the spatial evolution of the transport component.

To explain the dependency of hand aperture on arm transport, Haggard and Wing proposed a model that performs on-line error-driven corrections of a trajectory from a present position, P_i, to a target position, T_i. Coupling terms were assigned to express the effect of each component on the other's activity, as follows

$$\begin{bmatrix} \Delta P_{\mathrm{T}} \\ \Delta P_{\mathrm{A}} \end{bmatrix} = \begin{bmatrix} \alpha & \beta \\ \gamma & \delta \end{bmatrix} \begin{bmatrix} D_{\mathrm{T}} \\ D_{\mathrm{A}} \end{bmatrix},$$

where D_{T} is the difference between transport target position (T_{T}) and the current hand position (P_{T}); and D_{A} is the current difference between target aperture (T_{A}) and present aperture (P_{A}). ΔP_{T} and ΔP_{A} are increments in position that drive the states of transport and aperture towards their target states. The gains α, β, γ, and δ exert corresponding influence of each component over the other. α and δ are the influence that each component's D_i exerts over its own position change, whereas β is the influence that the aperture D_{A} exerts over the spatial state of the transport position, and γ is the influence that the transport component D_{T} exerts over the aperture component. Once the values of this gain matrix are chosen, they are fixed and the algorithm is executed iteratively, continuously updating D_{T} and D_{A}, and adding the corresponding increments ΔP_{T} and ΔP_{A} to P_{T} and P_{A}. Thus, remaining distances are exclusively used to drive the model variables towards their final states.

It is important to observe that the effect of reaching a maximum aperture larger than object size is achieved by the influence of the constant gain γ of the transport component's effect over the aperture component. This effect is larger when there is a large difference between present position and target position (at the beginning of movement), and subsequently decreases until the end of the movement, allowing the aperture to reach its target value—object size. With $[\alpha = 0.2;\ \beta = 0;\ \delta = 0.1;\ \epsilon = 0.2]$, this model provides a reasonable reproduction of the spatial plots of perturbed and unperturbed movement observed by Haggard and Wing. However, the model initiates with a velocity that is proportional to D_i, and, because of the constant gains, the increments ΔP_i are very large at the beginning and then low at the end. This makes the velocity profile unrealistic, with peak velocity long before 0.5MT, and with slow terminal approach of P_i to T_i. There is no time in this model, although there is iterated updating of current position.

An extension to this model produced somewhat more realistic velocity profiles (Atkeson & Hollerbach, 1985; Morasso, 1981). The model was extended to make target position and target aperture move from the initial P_{T} and P_{A} values to their final values at a constant velocity over the first 12 iterations (there were 30 iterations total). Thus the T_is were continuously updated and the P_is tracked those values. This transition was referred to by Haggard and Wang as an 'equilibrium trajectory' because of its relationship to the λ version of the equilibrium point model (Feldman, 1986). This modification produced more realistic velocity profiles, because as the P_is tracked the constantly increasing T_is, the momentary differences, D_is, were always small. This caused only small momentary increments in the present positions, thus avoiding the high initial velocities. The peak velocities for both aperture and transport were achieved when the equilibrium trajectory reached the targets T_is (12th iteration); from then on, the P_is slowly approached the T_is until the end of the movement. This extension to the model also generated larger apertures for faster movements, an effect already observed by Wing et al. (1986). However, it was not clarified how the additional equilibrium trajectory is generated by the brain.

2.6. Temporal equifinality of movement components using VITE

The vector operations in the Wing et al. model are similar to those utilized in the VITE (vector integration to end point) model of trajectory formation (Bullock & Grossberg, 1988a,b, 1991). The VITE model, however, is also capable of simulating an important property of prehension: synchronous ending of components, also known as 'temporal equifinality'. Additionally, in the VITE model, realistic velocity profiles are produced in a fundamentally different way than in the Wing et al. model. Moreover, the VITE model provides a basis for explaining synchronous ending of grip closing and hand/wrist transport. In a VITE circuit, different actuators in a movement can have different onset times, and still achieve temporal equifinality, provided that parallel channels are controlled by a common increasing gain signal. Fig. 6 shows the general working of the VITE model. In the blocks, vector components T_i represent the target position, P_i the current position, and D_i the difference between target and present position. A common gating signal $G(t)$ multiplies both components of the difference vector. D_i is integrated by P_i at a rate $G(t)$, which makes P_i continuously move towards T_i, until they have the same value, at which time D_i is zero and the movement stops. The use of $G(t)$ here allows temporal equifinality because P_i in each channel is updated at a rate that is proportional to the gating signal and to the difference between P_i and T_i. With a common gating signal that starts from zero at movement command onset and continuously grows as movement progresses, integration of all D_is finish approximately simultaneously, even if they do not start at the same time, because any D_i that starts late is multiplied by a larger mean $G(t)$ activation during its integration interval.

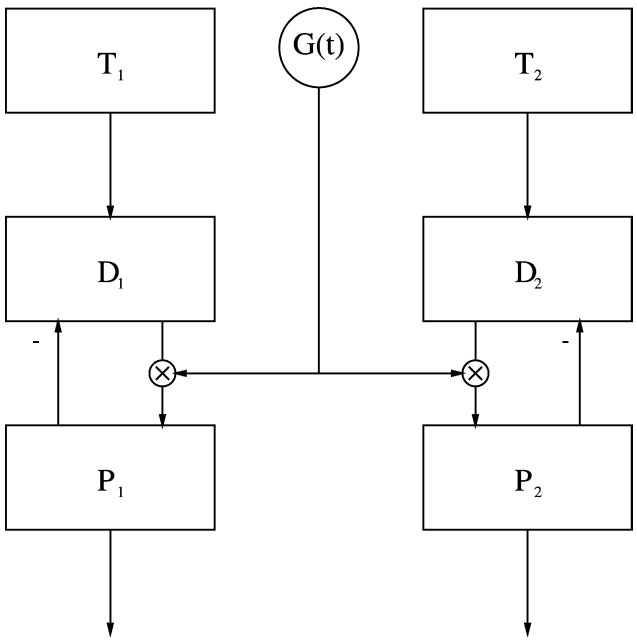

Fig. 6. Diagram of the VITE model. T_i, D_i, and P_i stand for target, difference, and present position vectors, respectively. A common increasing gating signal, $G(t)$, controls movement onset and rate, and allows temporal equifinality of both channels, even though they may start at different times and control movements of different amplitudes. Adapted from Bullock and Grossberg (1991).

A related property of the VITE model is its ability to compensate for a target switch on any channel after movement initiation. In this case, the switched target causes recomputation of D_i in the affected channel. The resultant D_i is then treated automatically like the late-starting D_i in the previous case. However, for sufficiently late target switches (or D_i onsets) the temporal equifinality property cannot be guaranteed unless the common GO signal is at least partially reset before resuming growth. Such partial reset also helps avoid abrupt and jerky direction reversals and has been used successfully in a prior application of the VITE model to serial 'viapoint' movements that require mid-course changes of direction (Bullock, Bongers, Lankhorst, & Beek, 1999).

The VITE model has been further developed beyond Fig. 6 structure to incorporate additional neuroanatomical connectivity and to explain aspects of load compensation (Bullock, Cisek, & Grossberg, 1998) and proprioceptive illusions (Cisek, Grossberg, & Bullock, 1998). This extended model's dynamic activity matches that of the neural firing pattern of predominant cell types in primary motor cortex (area 4) and parietal cortex (area 5), assessed during reaching tasks. Neurophysiological studies have revealed similarities between cortical cell activities during reaching and during grasping (Schwartz, 1994). In fact, both cortical areas have also been implicated in grasping (primary motor cortex: Donoghue, Leibovic, & Sanes, 1992; Lemon, Mantel, & Muir, 1986; Tanji, Kazuhiko, & Sato, 1988; and parietal cortex: Jeannerod, Arbib, Rizzolatti, & Sakata, 1995; Mountcastle, Lynch, Georgopoulos, Sakata, & Acuna, 1975; Taira, Mine, Georgopoulos, Murata, & Sakata, 1990). The GO signal was hypothesized in Bullock and Grossberg (1988b) to be generated in the basal ganglia. Consistent with that hypothesis, as well as the new coupling hypothesis introduced below, is the recent observation by Wenger, Musch, and Mink (1999) that pharmacological manipulations of the basal ganglia could reduce reaching speed and hand opening (maximum aperture), while leaving reach/grasp accuracy intact.

3. Methods

The planning problem in reaching and grasping coordination is how to ensure that the aperture and orientation rates are scaled to ensure completion in approximately the same time allowed by the transport phase. The coordination of these processes must be robust, so as to allow a natural adaptation when perturbations occur. A neural network model, based on the VITE model of trajectory generation of Bullock and Grossberg (1988a, b, 1991), was developed that reproduces key features of reaching and grasping coordination. A system of differential equations defines the circuit, depicted in Fig. 7. Transport, aperture, and orientation control modules work in parallel (cf. Contreras-Vidal, Ulloa-Perez, Lopez-Coronado, & Calabozo-Moran, 2001). The hypotheses of the new model are as follows:

1. Hand/wrist transport, grip aperture, and hand orientation are parallel and interdependent processes. Connections from both transport and orientation to aperture quantify the influence that transport velocity and orientation velocity have on the magnitude of grip aperture. Therefore, faster movements cause larger maximum grip apertures because transport and orientation velocity influence grip aperture magnitude.
2. Hand/wrist transport, grip aperture, and hand orientation are gated by a common internal GO signal, which enables synchronous completion of the reach–grasp components. No precomputation of component movement times is necessary.
3. Discrepancies between current perceived and internal representation of target positions are detected by cells that transiently inhibit the volitional GO signal, thereby avoiding jerky motions and preserving temporal equifinality despite unexpected changes in target location, target size, or target orientation.
4. Grip aperture evolves continually under the influence of a self-inhibition, due to passive biomechanical effects, that causes a tendency of the hand to close. This influence is especially manifested when there is

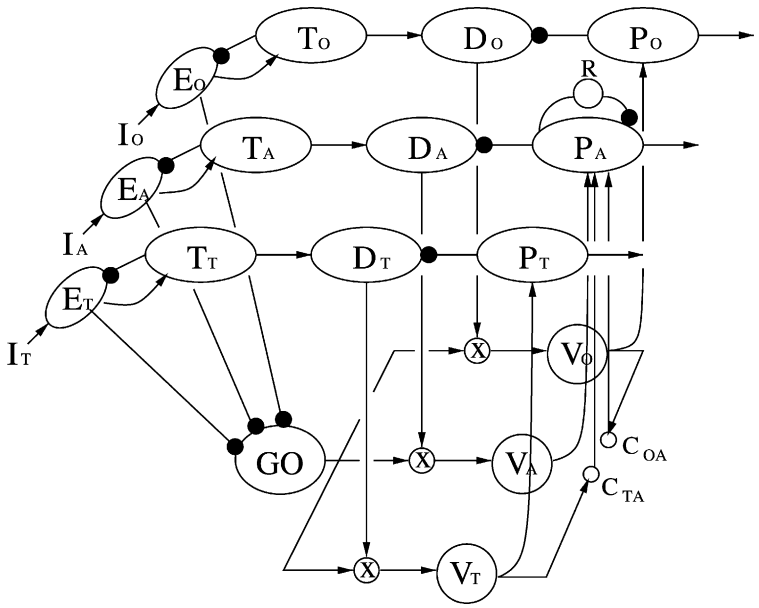

Fig. 7. Proposed model of reach–grasp coordination. T, D, and P stand for target, difference, and present position vectors, respectively; V is a velocity cell; the subscript indicates either transport (T), aperture (A), or orientation (O). During primed movements, D_is are allowed to grow to their full value before the GO signal gates the movement. T_T is object location, T_A is target aperture, and T_O is target orientation. I_i is the perceptual representation of the target for each component. E_i is the discrepancy between perceptual and internal representation of the target for each component. R represents a cell mediating delayed self-inhibition of hand aperture. C_{TA} and C_{OA} are cross-coupling influences from velocity of transport and velocity of orientation, respectively, to aperture formation.

no voluntary control acting on the hand, and is stronger for larger apertures.

3.1. Network structure

The proposed circuit, shown in Fig. 7, works as follows. The respective differences between ongoing values of the target parameters T_T, T_A, and T_O, and the desired values for these parameters that are specified by the currently perceived values of target location, target aperture, and wrist orientation, I_T, I_A, and I_O, are integrated by target cells, T_T, T_A, and T_O. Differences between present positions, P_T, P_A, and P_O, and target positions are registered in D_T, D_A, and D_O. Movement is initiated when the GO signal becomes active, triggering activation of velocity cells V_T, V_A, and V_O. The outputs of these velocity cells are integrated by their respective present position cells, but there is also influence from V_T and V_O over P_A. This cross-coupling, represented by C_{TA} and C_{OA}, is crucial for generation of maximum grip apertures that overshoot T_A, and the coupling had necessarily to be from velocity cells, given that maximum apertures should occur after 60% of movement time. Such timing of maximum grip apertures is achieved by the cross-coupling because velocity cells are active only after the GO signal has gated their activity, and they become maximal when transport and orientation velocities become maximal. Thus, this maximal activity influences, after some delay introduced by the cross-coupling cells, the aperture channel trajectory.

Fig. 7 shows that P_A, unlike P_T and P_O, is influenced by self-inhibition. This captures the hypothesis that the hand always tends to return to a semiclosed or relaxed position, even when there is no voluntary movement acting on the grip aperture. This tendency is interpreted as a biomechanical effect but implemented for simplicity as a delayed central self-inhibition (mediated by the cell R in Fig. 7) of present hand aperture, P_A. Cells E_T, E_A, and E_O represent discrepancies between perceived targets and internal representations of targets. If, after movement is initiated, any of the targets is modified, E_i cells will inhibit the GO signal, thereby slowing movement execution and allowing time for corrections. Also, when there is no target in any of the I_is, the corresponding T_i will remain equal to P_i. This allows independent execution of any module, that is, reaching without grasping or grasping without reaching.

3.2. Equations

3.2.1. Transport component

The transport component obeys the following system of equations

$$\frac{dD_T}{dt} = \alpha(-D_T + T_T - P_T), \tag{1}$$

$$\frac{dV_T}{dt} = \alpha_V(-V_T + G[D_T]^+), \tag{2}$$

$$\frac{dP_T}{dt} = V_T, \tag{3}$$

and

$$\frac{dT_T}{dt} = \alpha E_T, \tag{4}$$

where D_T is the transport difference vector, T_T is the internal representation of the position of the target, P_T is the transport present position vector, V_T is the transport velocity cell, G is the GO signal, and E_T represents the difference between perceived, I_T, and internal, T_T, representations of transport targets (Eq. (16)). The integration rate α was set to 30. This integration rate is used by most of the equations, except for the integration rate of velocity cells, α_V, which was set to 300.

3.3. Aperture component

The aperture component is represented by the following system of equations

$$\frac{dD_A}{dt} = \alpha(-D_A + T_A - P_A), \tag{5}$$

$$\frac{dV_A}{dt} = \alpha_V(-V_A + GD_A), \tag{6}$$

$$\frac{dP_A}{dt} = V_A + C_{TA} + C_{OA} - \phi R, \tag{7}$$

and

$$\frac{dT_A}{dt} = \alpha E_A, \tag{8}$$

where D_A is the difference vector for grip aperture, T_A is the internal representation of the target aperture, P_A is the aperture present position vector, V_A is the aperture velocity cell, C_{TA} is the influence that transport velocity exerts on aperture, C_{OA} is the influence that orientation velocity exerts on aperture (Eqs. (19) and (20)), and E_A represents the difference between perceived, I_A, and internal, T_A, representations of grip aperture targets (Eq. (17)). Note that P_A undergoes self-inhibition through ϕR, where $\phi = 3.5$, and

$$\dot{R} = \alpha(-R + P_A). \tag{9}$$

This inhibition accounts for the tendency of the hand to return to a relaxed (near zero) position. This tendency to close occurs even when there is no volitional movement on the aperture component, and it is stronger for larger grip apertures.

It is important to observe in Eq. (6) that D_A is not half-wave rectified, as opposed to D_T. This is a convenient simplification. Neural signals are typically half-wave rectified, and the present simplification could be replaced by a push–pull arrangement of two oppositely polarized half-wave rectified D_A processes, as implemented in some other versions of VITE.

3.4. Orientation component

The orientation component is represented by the following system of equations

$$\frac{dD_O}{dt} = \alpha(-D_O + T_O - P_O), \tag{10}$$

$$\frac{dV_O}{dt} = \alpha_V(-V_O + G[D_O]^+), \tag{11}$$

$$\frac{dP_O}{dt} = V_O, \tag{12}$$

and

$$\frac{dT_O}{dt} = \alpha E_O, \tag{13}$$

where D_O is the difference vector for the orientation component, T_O is the internal representation of the target orientation, P_O is the present orientation vector, V_O is the orientation velocity cell, and E_O represents the discrepancy between perceived, I_O, and internal, T_O, representations of orientation targets (Eq. (18)). Note that the orientation component was introduced to account for studies on target orientation perturbation (Paulignan et al., 1991b). If target orientation remains unaltered in a grasping task, the orientation component stays inactive—and, therefore, has no effect on aperture formation.

3.5. GO signal

The GO signal was defined in the following way

$$\frac{dG}{dt} = \alpha_G(-G + G_0(t) - G(\gamma E_T + \delta E_A + \epsilon E_O)), \tag{14}$$

where

$$G_0(t) = g_0 t^{1.4}, \tag{15}$$

and $\gamma = 5$, $\delta = 15$ or 1, $\epsilon = 10$, g_0 is the GO amplitude, and $\alpha_G = 300$. G is the GO signal multiplying the difference vector of each component, and G_0 is a function of time since the onset of step input g_0 from a decision center in the brain. The two different values of δ correspond to two different object-size perturbation cases. However, the value of δ to be used depends entirely on initial object size, in a block of trials in which a change can only be made either from small to large or from large to small. In the simplified application of δ in the present simulations, if the initial object is small, a δ of 15 is used, because the only possibility left is a change from the initial small object to a large one. When the initial object is a large one, a δ of 1 is used, because the only possibility left is a change from the initial large object to a small one. When an object is increased in size, the effect that this change has on movement speed is larger than when the object size is decreased. Only in the case where the object size is increased is there an increased risk of collision of the fingers with the object, due to too little aperture. Signals E_T, E_A, and E_O are outputs of cells that register

the discrepancies, if any, between current target parameter values and perceived targets. When location, orientation, or size of targets are altered during reach to grasp execution, the E_i signals allow such alterations to inhibit the GO signal momentarily, thereby slowing down the movement in proportion to current GO value and therefore modulating the ongoing movement. Thus, movement time is lengthened whenever such disturbances occur. It is important to mention that there are two types of coupling in the model: direct coupling, which is implemented by explicit state coupling terms in the aperture equations; and indirect coupling, which is mediated via effects of state coupling in the GO signal equations.

3.6. Discrepancies between perceived and internal targets

The discrepancy cells were defined by

$$\frac{dE_T}{dt} = \alpha(-E_T + \text{abs}(I_T - T_T)), \tag{16}$$

$$\frac{dE_A}{dt} = \alpha(-E_A + \text{abs}(I_A - T_A)), \tag{17}$$

and

$$\frac{dE_O}{dt} = \alpha(-E_O + \text{abs}(I_O - T_O)). \tag{18}$$

3.7. Coupling neurons

The coupling neurons were defined by

$$\frac{dC_{TA}}{dt} = \alpha(-C_{TA} + \rho V_T), \tag{19}$$

and

$$\frac{dC_{OA}}{dt} = \alpha(-C_{OA} + \sigma V_O), \tag{20}$$

where $\rho = 0.5$ and $\sigma = 0.5$. The coupling from V_T and V_O to P_A causes a maximum aperture that exceeds object size and scales with transport velocity and orientation change velocity.

4. Results

4.1. Basic features of prehension

To test our model's ability to simulate the basic qualitative features of prehension, a reach–grasp movement experiment by Paulignan et al. (1991b) was simulated. In this experiment, subjects were instructed to reach for an object of 1.5 cm diameter. The distance between initial and final position was 36 cm. The plots in the right column of Fig. 1 show simulations of the reaching and grasping movements from the experiment by Paulignan et al. (1991b). The model reproduced the basic features of a normal prehension movement, as shown in the data plots shown on the left side of Fig. 1. Transport velocity exhibits an approximately bell shaped velocity profile typical of point-to-point arm movements (Bullock & Grossberg, 1988a; Nagasaki, 1989). The plot of hand aperture shows the hand opening to its maximum aperture, then decreasing until it reaches object size. Both transport and aperture end synchronously. It is important to note that the bell shape of the wrist velocity profile is only approximated by the multiplication of the transport difference vector by the GO signal used here. The generation of a GO signal to be used for transport trajectory generation is only a representation of a real gating signal, believed to be controlled by the basal ganglia (Bullock et al., 1998; Bullock & Grossberg, 1988b, 1991). It is beyond the scope of this paper to offer an elaborated explanation of its generation.

4.2. Maximum aperture overshoots

To observe the dependency of the grip aperture overshoots on the cross-couplings from velocity of transport to grip aperture evolution, the basic reach–grasp experiment of Paulignan et al. (1991b) was simulated with no cross-couplings. Fig. 8 (left column) shows the absence of hand aperture overshoots when the model is run with zero cross-couplings. In other words, in the model, the hand aperture overshoots are entirely attributable to the cross-couplings.

4.3. The synchronizing role of a growing GO signal

To observe the extent to which synchronization of the components of reach–grasp depend on a growing GO signal, the basic reach–grasp experiment of Paulignan et al. (1991b) was simulated with a constant GO signal (GO = 8). A comparison of Figs. 1 and 8 (right column) demonstrates the synchronizing role of an increasing GO signal. In the simulation plotted in Fig. 8, the increasing GO signal used for Fig. 1 was replaced by a GO signal of constant value. As can be observed in the figure, there is very poor coordination of transport and aperture components when the GO signal is constant-valued. The transport velocity component does not show the bell-shape velocity profile typical of point-to-point arm movements. Also, the transport component finishes after the aperture component is completed, as can be appreciated by comparing termination times of upper and lower plots in Fig. 8. Coordination would be even worse if either component were perturbed or if onsets were staggered.

4.4. Zero vs. large initial apertures

To show that our model is capable of reproducing partial grip closures that occur when the hand grip aperture starts at a sufficiently open position, the experimental data of Saling et al. (1996) was simulated. The simulations are shown on

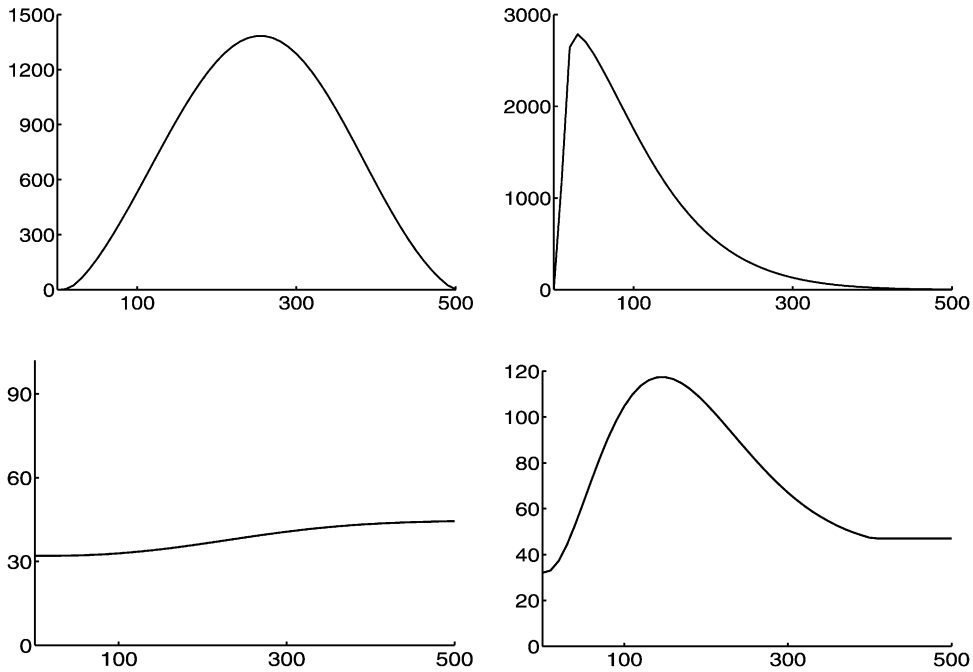

Fig. 8. Left column: Simulations of transport velocity (upper) and grip aperture (lower) using zero cross-couplings. The absence of hand aperture overshoots when the model is run with zero cross-couplings shows that the hand aperture overshoots (visible in other figures) are entirely attributable to the cross-couplings. The hand aperture plot was shifted by 3.2 cm to match the shift in position included in the data plots (see explanation in Fig. 1). Right column: Simulation of a grasping movement using a constant GO signal. Even in the case where neither component is perturbed, there is poor coordination of transport (upper) and aperture (lower) components when the GO signal is constant-valued. In this case, a constant value of 8 was assigned to the GO signal. Compare to Fig. 1, in which an increasing GO signal was used.

the right-hand side of Fig. 2. The corresponding data plots are on the left-hand side of the same figure. Continuous lines represent normal grasping movements, and dashed lines movements with altered initial hand aperture. A normal grasp initiates with an aperture of zero, and an altered grasp initiates with an aperture larger than zero (11 cm in the plots of Fig. 2). Object sizes were 2.2 and 6.7 cm. The object was located at 30 cm from the subject. GO amplitude was set to 45. In the simulation of altered hand apertures of Fig. 2, as in the data in the same figure, a partial closure can be observed, followed by a reopening, and finally the target enclosure. Note that the simulated velocity profiles of hand aperture are suddenly interrupted when the aperture reaches object size. This interruption of the aperture formation was introduced to correct for the lack of rectification in the difference vector of the aperture component. In the model, the difference vectors of transport and orientation are half-wave rectified before multiplying the GO signal (Eqs. (2) and (11)), whereas the difference vector for aperture is not (Eq. (6)). Therefore, the difference vectors in transport and orientation equal zero after they have reached or overshot their respective targets. In the aperture component, however, the lack of rectification in the aperture difference vector creates oscillations around the aperture target. To prevent these oscillations from happening in the simulations, the integration of hand aperture position was stopped when hand aperture achieved its target (or contacted the object). This stopping of the aperture formation made sense since the hand aperture cannot grasp beneath the object surface, and the velocity of aperture should become zero after contacting the object surface. This is reflected in the simulation plots by a fast drop of the aperture velocity profile to zero, once the aperture formation becomes equal to object size.

4.5. Perturbations to object location/orientation

To show that our model is capable of simulating adaptation to perturbations of object location/orientation, the data of Paulignan et al. (1991b) was simulated. In the model, simulations show an elongation of movement time when the location of the targeted object is changed at movement onset. Simulations of grasping when object position is perturbed (Paulignan et al., 1991b) are shown on the right-hand side of Fig. 3. The corresponding data plots are shown on the left-hand side of the same figure. The figure shows transport and aperture kinematics when a 1.5 cm cylindrical object's position was unexpectedly shifted, at movement onset, from 20 to 30° with respect to the body midline. As a result of this shift, the object's distance from the subject changed from 35 to 34 cm. The two upper rows illustrate transport tangential velocity and hand aperture for an unperturbed grasp; the two lower rows illustrate transport tangential velocity and hand aperture for the perturbed case. Note that the hand aperture plot of the simulation was shifted by 2.2 cm to match the data plots, in

which the initial hand aperture was 2.2 cm. This was because the finger-mounted markers recorded by the camera were not at the fingertips.

To reflect the differences in the accelerative phases of the upper and lower data plots, the GO amplitude was set to 45 for the upper simulation and to 80 for the lower simulation. This change accounts for the observation of Paulignan et al. (1991b) that the velocity peak of the first submovement in the perturbed trials was achieved earlier than the velocity peak in the unperturbed trials.

For unknown reasons, the velocity traces in the left column of Fig. 3 do not start at zero (although other plots in the same publication do start at zero). Without the left tails of these velocity profiles, they appear to be more asymmetrical than one would expect from other published profiles (Bullock & Grossberg, 1988a,b; Nagasaki, 1989; Zhang & Chaffin, 1999). By being more symmetrical, the model velocity traces in the right column appear to mismatch the data, but it is expected that this would not be true of a comparison with the complete velocity profiles, were they available.

Note that in Fig. 3, there is a discrepancy between data and simulation plots of the grip aperture unperturbed case. In the data plots, the initial portion of the aperture does not monotonically increase towards maximum hand aperture, as in the simulation. This seems to be an anomaly in the particular data trial shown, since it was not present in other hand aperture data plots. A good match is obtained in other cases, such as in Fig. 1.

Another discrepancy between data and model can be appreciated by comparing the peaks of the data and simulation of the second submovement of the transport velocity, perturbed case. In this case, the transport velocity trace, after adjustment to the perturbation has started, is smaller in the data plot than in the simulation plot. This is due to the growing effect of the GO signal in the model, even after it was transiently inhibited. However, in both data and simulations, the movement duration is lengthened by similar amounts. Paulignan et al. (1991b) reported an average lengthening of MT by 100 ms on average (although this is not apparent from a comparison of the particular control and perturbed trials shown). When the perturbation was registered by the model at $t = 180$ ms, to reflect a visual processing delay, such a lengthening also occurred in the model.

In order to illustrate the internal working of the model for location perturbation, plots of internal variables for this perturbation are shown in Figs. 9 and 10 for the unperturbed and the perturbed cases, respectively. In both figures, the first column represents variables of the transport component, except for the last plot in that column, which shows the evolution of the GO signal. In the second column, variables are shown that correspond to the aperture component. In the third column, variables are shown that

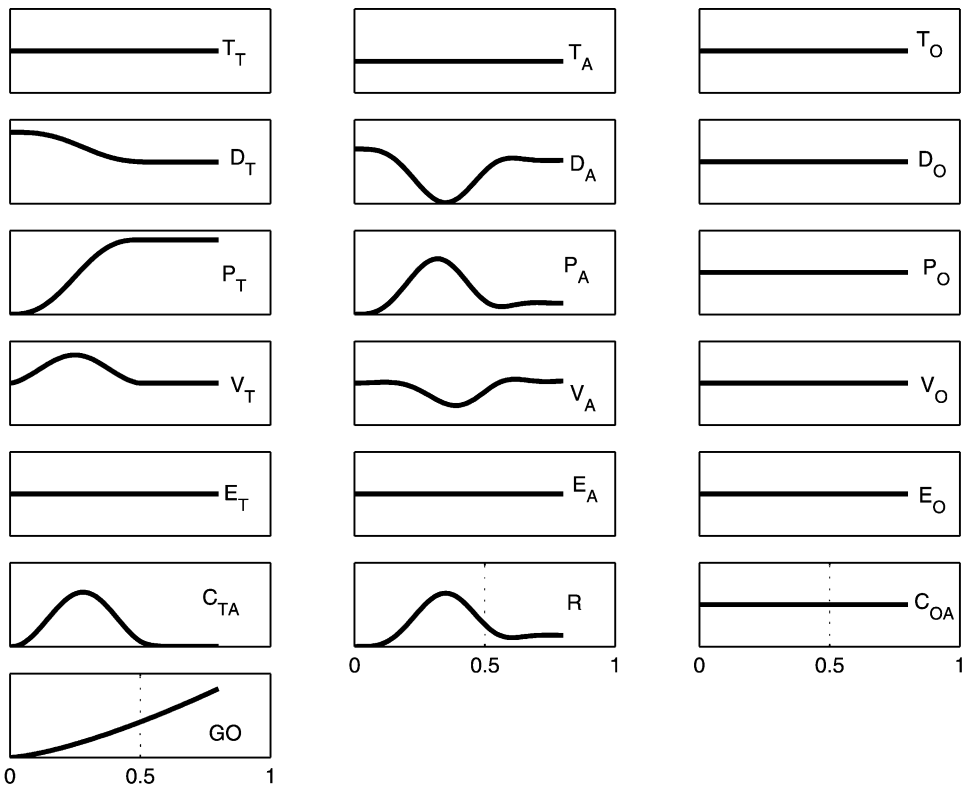

Fig. 9. Illustration of internal variables in the reaching and grasping coordination model, for an unperturbed grasping movement. Names of variables as in Fig. 7.

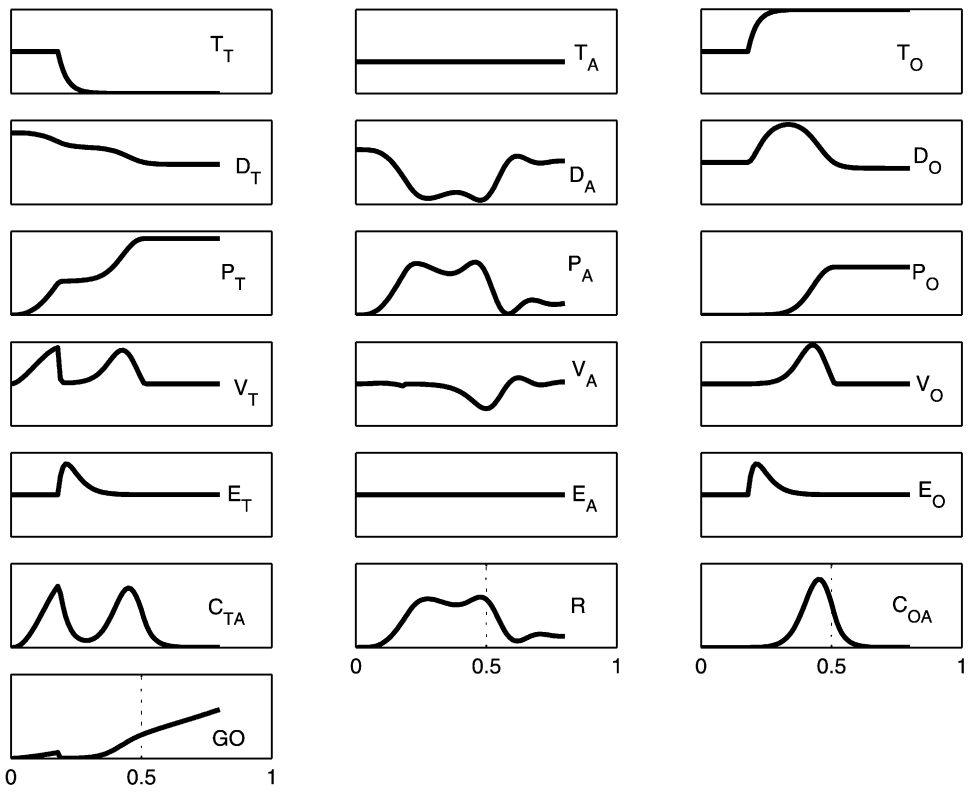

Fig. 10. Illustration of internal variables in the reaching and grasping coordination model, for a grasping movement in which the object location was perturbed at movement onset. Names of variables as in Fig. 7.

correspond to the orientation component. In Fig. 9, which shows an unperturbed grasping movement, the variables in the orientation component remain at zero, given that there was no activity in this component (no orientation target change was instantiated). A target for transport, $T_T = 35$ cm, and a target for aperture, $T_A = 1.5$ cm, are instantiated, which generate corresponding difference vectors, D_T and D_A. These difference vectors, gated by the GO signal, are integrated by their respective present position commands, P_T and P_A, thus generating movement in each channel. Velocity cells, V_T and V_A, are also shown for each component, as well as discrepancy cells, E_T and E_A, which equal zero given that no perturbation in targets was instantiated. However, the cross-coupling from velocity of transport, C_{TA}, influences the grip aperture, thereby generating a transient aperture overshoot in P_A. Plot of variable R shows the self-inhibition that tends to relax the aperture of the hand.

Fig. 10 shows the internal variables of the model for the location perturbation case presented in Fig. 3. In this figure, the orientation component does show activity, given that a target (a reorientation) was instantiated in this component for the perturbed case. A target for transport, T_T, is instantiated to 35 cm. A target for aperture, T_A, is instantiated to 1.5 cm. These two targets are known before movement initiation, so that a difference vector can be obtained. The orientation target, T_O, remains at zero before movement onset. Movement is initiated towards transport and aperture targets, and trajectories are generated for transport and aperture. At $t = 180$ ms (a delay due to visual processing), new targets are presented to the perceptual input units (not shown) of the model for transport and orientation, $I_T = 34$ cm, and $I_O = 10°$. These changes generate discrepancies between internal representations of targets, T_T and T_O, and perceptual targets, I_T and I_O. These discrepancies are registered by cells E_T and E_O, for which a sudden burst of activation is shown in Fig. 10. The activity in E_T and E_O inhibits the GO signal, which partially resets its activity. As the activity in E_T and E_O vanishes, the GO signal gradually resumes its normal evolution. The activity in E_T and E_O decreases towards zero as the discrepancies are gradually integrated by T_T and T_O. Since the GO signal was partially reset, the overall movement takes longer to complete. The aperture formation, P_A, is also affected by the perturbation, by virtue of the cross-couplings C_{TA} and C_{OA}.

4.6. Perturbations to object size

To show that our model is capable of simulating adaptation to perturbations of object size, the data of Paulignan et al. (1991a) was simulated. Simulation results of grasping when object size was unexpectedly perturbed (Paulignan et al., 1991a) are shown on the right column of Fig. 4. The corresponding data are shown in the left column

of the same figure. The data plots show a representative experimental trial for one subject. Aperture velocity is indicated by a dashed trace, aperture itself by a heavy trace. Object sizes were 1.5 and 6 cm. The target object was at a distance of 35 cm. GO amplitude was set to 40. Note that the hand aperture plot was shifted by 5 cm to include the shift in position of the data plots. This shift is due to the position of the markers on the fingers. The parameter δ was changed from 15 to 1 in the LARGE-TO-SMALL perturbation, on the assumption that when the change is made from a large to a small object, the discrepancy has a smaller effect on inhibiting the GO signal than during a SMALL-TO-LARGE perturbation. Only in the case of a SMALL-TO-LARGE perturbation are the fingers at risk of collision with the object due to too little aperture. The perturbation was registered by the model at $t = 200$ ms (not 180 ms, cf. location perturbation), based on data indicating slower visual processing in the object size than in the object location streams (Tannee, Boussaoud, Boyer-Zeller, & Rouiller, 1995).

4.7. Model performance for a range of GO amplitudes and object sizes

The model was tested for a full range of GO amplitudes and object sizes. Transport was considered to be complete when hand/wrist velocity was less that 0.05 cm/s. Aperture formation was considered to be complete when the aperture size equaled object size. Enclose time was calculated as the time from maximum aperture to hand closing (Zaal et al., 1998). These criteria used for testing the model were a compromise among the various criteria used by experimenters. For instance, Zaal et al. (1998) marked initiation of movement when the arm velocity reached 5 cm/s, and movement completion when the velocity of the aperture was less than 7.5 cm/s. Castiello, Stelmach, and Lieberman (1993), on the other hand, defined transport onset as the time when transport displacement was greater than 0.3 mm, and grasp onset as the time when thumb-finger distance increased 0.3 mm from the starting aperture. Castiello et al. defined movement time as the time from transport initiation to grasp end (i.e. when thumb-finger distance was equal to object size). With this in mind, it is expected that a single criterion, such as the one used here, will not fit perfectly all experimental observations. However, the model should be consistent with empirical trends when varying GO amplitudes and object sizes over full experimental ranges.

For a full range of GO amplitudes, the model shows consistent relative timing of maximum apertures. Fig. 11 shows the timing of reach–grasp components over various simulations using a full range of GO amplitudes. Increments of the GO amplitude increase the speed at which the grasp is made. However, the relative timing of occurrence of maximum aperture (64.6–70.8%) is maintained over the range of speeds.

Fig. 11 shows another data-consistent property of the model: larger maximum apertures for faster movements (Wing et al., 1986). Fig. 11 shows a maximum aperture of 5.38 cm for the slowest of the movements simulated (GO

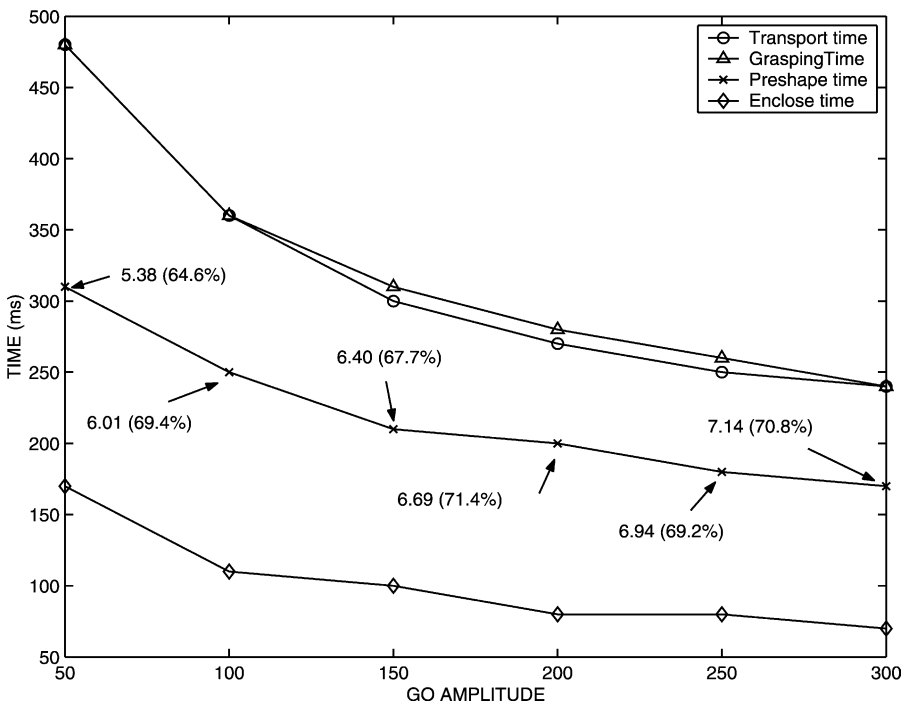

Fig. 11. Durations of transport, grasp, preshape and enclose for a range of GO amplitudes. The numbers around the preshape time graphs correspond to maximum hand aperture (in cm) and time of occurrence of maximum hand aperture with respect to transport time (in parenthesis). Transport distance was set to 24 cm, object size was 2.2 cm. The transport phase was considered terminated when it was less than or equal to 0.05 cm/s.

amplitude of 50). This maximum aperture gradually increases as the speed of the movement increases. For the fastest movement (GO amplitude of 300), a maximum aperture of 7.14 cm is obtained. The larger maximum apertures for faster movements are obtained in the simulations by the cross-coupling effect from transport velocity and orientation velocity, which influence aperture formation, thereby generating a transient overshoot in aperture. This overshoot is larger when velocity of transport and velocity of orientation are larger. Because of the speed-accuracy tradeoff in human movement (Fitts, 1954), faster movements will always be less accurate than slower movements. Thus the error in movement scales with velocity of movement. The functional effect of the overshoot in hand aperture is to provide tolerance for error in movement (transport or orientation), and is useful to avoid collisions of the fingers with the targeted object (Haggard & Wing, 1995).

For a full range of object sizes, the model shows consistent relative timing of maximum apertures. Fig. 12 shows the timing of the components of grasping when simulations were run over a full range of experimental object sizes. This range of sizes was chosen because 0.3 and 8 cm were, respectively, the smallest and largest objects found in the reach–grasp literature. As in the previous figure, the relative timing of maximum aperture ranges (60.0–79.1%) show consistency with values found in the literature. However, there is another trend. The time of maximum aperture increases with object size whereas the enclose time decreases. This is in accord with an observation of Hofsten and Ronnqvist (1998). Also, Castiello et al. (1993) observed that when grasping objects of different sizes, the maximum grip aperture occurs later for a larger object. Since occurrence of maximum aperture marks the beginning of the enclose time, it is possible to consider Castiello et al.'s observation as implying that enclosing times are longer for smaller objects, which confirms the above studies and the simulations.

This interpretation, and the simulation results, are in accord with the empirical rule of thumb recently proposed by Mon-Williams and Tresilian (2001) to summarize relative durations of opening and closing phases as a function of object size. If equifinality of reach and grasp components were obeyed equally for all object sizes, then the shorter enclose times could be wholly attributed to the later times of maximum aperture observed for larger objects (since enclose time, by definition, begins at the time of maximum aperture). However, Fig. 12 reveals that the model exhibits a progressive deviation from equifinality as object size increases. In the model, this deviation is the larger contributor to the inverse relation between enclose time and object size. This deviation is in turn attributable to the self-inhibition term (R) in grip aperture, which is larger for larger apertures and which acts to accelerate grip closure and shorten enclose time independently of the difference vector (D_i) or GO signal. Another consequence of the same self-inhibitory factor is that although the maximum aperture increases linearly with object size, the slope (at 0.67) is less than one, so the aperture overshoot is significantly less for a large than for a small object.

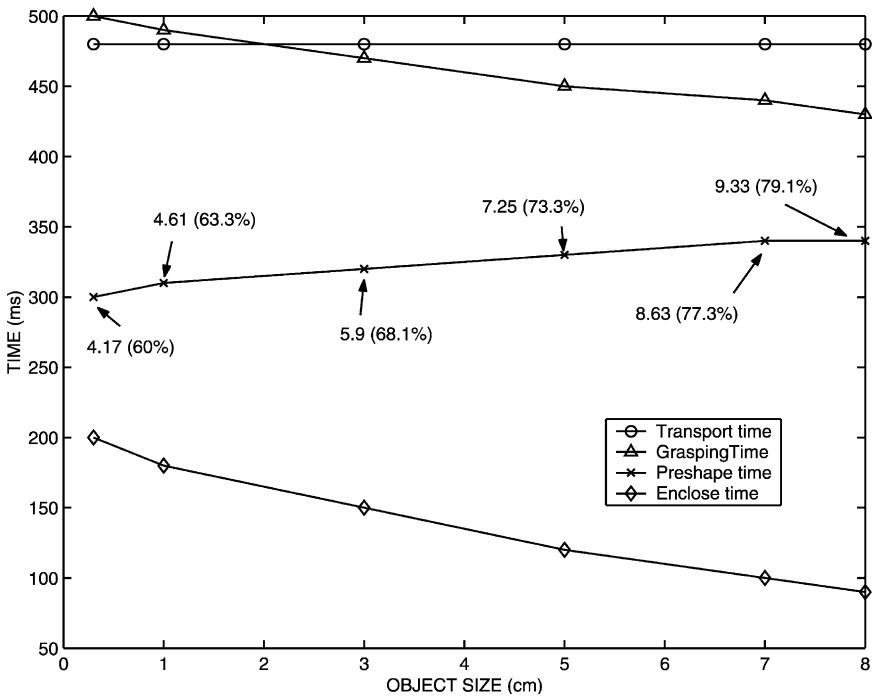

Fig. 12. Durations of transport, grasp, preshape and enclose for a range of object sizes. The numbers around the preshape time graphs correspond to maximum hand aperture (in cm) and time of occurrence of maximum hand aperture with respect to transport time (in parenthesis). Transport distance was set to 24 cm. GO amplitude was set to 50.

In particular, there is a maximum aperture of 4.17 cm for a 0.3 cm object. A maximum aperture of 9.33 cm is obtained for an 8 cm object (the largest object simulated). Thus the aperture overshoot per se is much larger for the smallest object than for the largest object (3.87 cm for the 0.3 cm object, and 1.33 cm for the 8 cm object). Note that despite the self-inhibition term on aperture formation, the model is still capable of achieving maximum grip apertures larger than the object for larger objects.

Different object sizes always yielded the same simulated duration for transport. Although it has been reported that wrist movement times are longer for larger objects (Jakobson & Goodale, 1991), in that study transport was considered to be ended at the time at which the object was lifted, not at the time of first contact. In contrast, Bootsma, Marteniuk, MacKenzie, and Zaal (1994) reported that object size does not systematically influence transport time. Bootsma et al. established the end of the movement as the first direction reversal in hand displacement. This criterion appears to better reflect the transport component than the criterion used by Jakobson and Goodale. Hence, according to the results of the model, it is hypothesized that wrist movement durations are not necessarily influenced by object size.

5. Discussion

5.1. General findings

Successful prehension across a wide range of contexts requires adaptive coordination between the different task/end-effector degrees of freedom that contribute to the act. Across acts of prehension, objects of grasp can change in their positions relative to the body, their orientations relative to the body, their sizes, their shapes, and their mechanical properties, such as surface friction, compressibility and mass distribution. In this paper, the focus has been on three aspects of the kinematic control and coordination problems—transport, orientation, and aperture—that, respectively, arise from object variations in position, orientation, and size. It was argued that VITE-type trajectory generators based on gated integration of difference vectors computed between desired and current states could provide the fundamental competence needed to adapt to the three types of object variations addressed.

Our reach–grasp model was shown to be in accord with empirical observations of prehension. Specifically,

- the components of prehension were synchronized, a consequence of having a common scalar gating signal whose magnitude grows during the movement interval;
- the transport velocity exhibited a unimodal and symmetrical velocity profile typical of point-to-point arm movements, a property already demonstrated by the VITE model;
- maximum grip aperture occurred at 60–80% of movement time, a property accomplished by the delayed effect of influences of transport and orientation velocities on aperture formation;
- maximum grip aperture was larger for larger objects, since a larger present aperture command is added to the cross-coupling influence for larger object sizes;
- maximum grip aperture was larger for faster movements, due to influences of transport and orientation velocities on aperture formation;
- movement time increased when any component of prehension was perturbed, due to the inclusion of discrepancy cells which inhibited the common gating signal during perturbations;
- grip aperture decreased when the hand started open more than a certain magnitude or when movement paused, due to the introduction of a self-inhibition, attributed to a biomechanical effect but modeled as a central effect;
- enclose time was shorter for larger objects because the aperture overshoot was less for larger than for smaller objects.

5.2. Model–model comparisons

Any three controllers acting on a single system like the hand-arm are of necessity coupled by mechanical interactions if they are sensitive to evolving feedback signals. However, in this study, such interactions were ignored in order to focus on the question of what internal couplings, within the command system itself, could serve as a basis for robust responses to object variations. In principle, multiple controllers acting in parallel could be spatially coupled, temporally coupled, or both. Moreover, such coupling could occur only at selected times, or continuously. In the Zaal et al. (1998) dynamical model, a temporal coupling from transport to aperture continuously geared the hand aperture to time-to-contact information with the object, but no spatial trajectories were generated. In the Hoff and Arbib (1993) model, there was no spatial coupling, and the temporal coupling occurred only prior to movement onset. In the Haggard and Wing (1995) model, there was continuous spatial coupling but no temporal coupling.

The model proposed here employs continuous temporal and spatio-temporal (velocity) coupling, and in that sense adopts ideas from the Hoff and Arbib and the Haggard and Wing models. However, using the VITE generator as a basis allowed a solution that eliminated any need for pre-computation of component times (as in the Hoff and Arbib model) or for a two-stage construction of realistic velocity profiles (as in the Haggard and Wing model). In particular, temporal coupling was achieved by using a common GO signal to control the onset, perturbation-induced slowing, and normative speeding of the vector integration process in all three controllers. Provided that this GO signal grows during

the prehension movement, it provides a powerful basis for temporal equifinality of the controller cycles, and thus for synchronous termination of transport, hand reorientation, and aperture closure to grasp the object. The synchronizing property of a growing GO signal is particularly important for staggered onset times or, as occurs in the current simulations, when one of the channels is transiently perturbed from its normal evolution. A growing GO signal multiplied by the residual difference vector in the channel which is farther from its target will produce more movement in that channel than in the channels that are closer to their target, thereby allowing the late-starting or perturbed channel to catch up with the evolution of the rest of the channels. A notable property is that this design easily and automatically compensates for variability in sensory processing delays. For example, it can autocompensate if, as reported empirically, the pathway computing object location is faster than that computing object size.

Regarding spatial coupling, the present simulations confirm that there is no need, as in the Hoff and Arbib model, to sequentially program separate 'maximum' and 'final' apertures for the grip. Instead, it sufficed to allow the transport and orientation velocity control signals to have a proportionate effect on the grip aperture, in a manner similar to that introduced in the Haggard and Wing model. Spatial cross-coupling via these signals naturally causes a transient grip aperture overshoot that is larger in movements with faster transport or faster reorientations. Both compensations serve the purpose of helping to avoid contact of the hand with the object before the fingers are ready to close upon it. The speed-accuracy tradeoff that characterizes all movements implies that fast transport or reorientation movements will be less accurate. This reduced accuracy raises the risk of hand collision with the object 'on the way in', a risk that can be avoided by increasing aperture.

Because hand/wrist position and hand orientation affect the grip aperture significantly, but not vice-versa, there was no reason to introduce reciprocal links from aperture velocity to the other two controllers. Thus the model connectivity is not symmetrical. Another aspect of broken symmetry in the model is the assumption of a spontaneous relaxation of the aperture to a closed resting position. Although implemented nominally as a central process, our thesis is that it reflects a passive biomechanical factor. Such passive closure seems more natural than active closure as an explanation of the transient early overshoot of aperture reduction in the 'altered' trials of Saling et al. (1996).

These simple provisions for temporal and spatio-temporal coupling allowed the model to recreate all the cited empirical trends regarding aperture size variations and relative timing of maximum aperture vis-a-vis the transport movement time. Moreover, the model was able to provide a good approximation of the qualitative dynamics exhibited by the full range of movements treated.

5.3. Brain areas involved in grasping and reach–grasp coordination

Areas of the brain related to the reaching component of the VITE model have been reviewed elsewhere (Bullock et al., 1998; Cisek et al., 1998). Those reviews emphasized primary motor and parietal cortex, both of which are also implicated in the execution of precision grasping. The hand area of primary motor cortex can be associated with the present position aperture in our model and the hand area of posterior parietal cortex with the aperture difference vector in our model. Reversible inactivation of the motor cortex hand area in monkeys produces an inability to grasp using the contralateral hand (Fogassi et al., 2001), and changes of firing frequency of cortico-spinal neurons in motor cortex area 4 have been shown to produce facilitation of hand muscles in monkey (Lemon & Mantel, 1989). In humans, fMRI studies show activation of primary motor cortex during grasping movements (Ehrsson et al., 2000). Reversible inactivation of the anterior intraparietal hand area in monkeys produces a disturbance in hand preshaping using the contralateral hand (Gallese, Murata, Kaseda, Niki, & Sakata, 1994). In humans, lesions in posterior parietal cortex produce deficits in matching hand opening with object size (Jeannerod, Decety, & Michel, 1994). Regarding hand orientation during grasping, lesions of the monkey's area V6A in posterior parietal cortex generate deficits in wrist orientation during grasping tasks (Battaglini, Muzur, Galleti, Skrap, & Fattori, 2002).

The model's couplings, from velocities of orientation and transport to aperture, could be mediated by several pathways. Perhaps the most likely is an adaptive trans-cerebellar pathway. Such a pathway would involve an efference copy of the desired velocity vector in motor cortex. This efference copy would be carried by a cortico-pontine projection to cells of origin for mossy fibers that would enter the cerebellum. The velocity vector would thus serve as the basis for a cerebellar representation of state, which would serve as a dynamic context for the generation of cerebellar adjustments to hand aperture. Unwanted contact of the fingers with the object could serve as an error signal that could help train the cerebellum to adjust the amount of opening to reflect the transport velocity. The cerebellar output could act via aperture position controllers in motor cortex. This proposal is consistent with data indicating that cerebellar loops that exist between primary motor cortex and cerebellum can modify externally guided movements (see Middleton & Strick (2000) for a review). In fact, we have recently developed a model that uses a similar adaptive pathway to adjust grip force to prevent the slip of objects from the hand (Ulloa, Bullock, & Rhodes, 2003).

6. Conclusions

The properties of reaching and grasping were simulated with an extension of the VITE model for arm movements. The present model intended to achieve coordinated activity in channels controlling arm transport and those controlling hand aperture, as well as the scaling of those components to achieve simultaneous termination of both. A third component, not usually considered in the experimental literature, was introduced in order to reproduce a portion of the data on perturbations: hand orientation, which quantified the change in wrist orientation with respect to the arm. In the new model, the timing of the three components was coordinated by using a common gating signal. This common gating allowed the coordination to be robust and permitted natural adaption to perturbations.

Because this model is an extension of the VITE model for arm movements, the performance of the new reaching and grasping model showed how a biologically based neural network is capable of modeling online coordination in reaching to grasp static objects. This circuit for reaching and grasping coordination explains various aspects of experimental observations of reaching and grasping. The model follows principles of biologically based neural models and, consequently, is consistent with pertinent constraints from primate neurobiology.

7. Future research

The purpose of the present model was to extend the VITE model of trajectory generation to simulate the coordination of reaching and grasping in prehension. Based on this precept, it is a future task to make predictions based on the functioning of the current circuit, as well as sensitivity analyses, e.g. can the model explain the variation around the two-thirds relative timing of maximum aperture? To explore these and other alternatives, further simulations can be conducted.

An interesting variant of the model is to investigate whether it can explain coordination of reaching and grasping when the target object is moving. In this particular problem, there may or may not be a transport component to synchronize with grip aperture, because the object could be on a collision course with the stationary hand. In this case, it is necessary to make grip opening and closing rates accelerable by a contact imminent signal (Bullock et al., 1999), which is the reciprocal of a time-to-contact signal. Thus a time-to-contact dependent signal could be included in the circuit for reaching to grasp a moving object, in which case the GO signal will be sped up when contact becomes imminent.

A VITE-like model has already been used to simulate interception of moving objects (Peper, Bootsma, Mestre, & Bakker, 1994). Peper et al.'s model adequately used time-to-contact information to continuously control the trajectory of hand movement. Another paper (Dessing, Bullock, Peper, & Beek, 2000) reported further successes in using VITE as a basis for simulating reaching to intercept objects approaching the actor on various trajectories. However, neither of these treatments had dealt with the grip aperture control and transport–aperture coordination treated in the present paper, both of which are necessary to grasp a moving or stationary object such as a ball. Future work could undertake a combination of the current model with that of Dessing et al. to more fully model temporal dynamics of one-handed ball catching. If successful, the final step would be to use the neural network model to control a 3D arm-hand model that incorporates realistic mechanical degrees of freedom.

Acknowledgements

Antonio Ulloa was supported by Consejo Nacional de Ciencia y Tecnología of México (CONACYT 65907). Daniel Bullock was supported in part by DARPA/ONR N00014-95-1-0409.

References

Atkeson, C., & Hollerbach, J. (1985). Kinematic features of unrestrained vertical arm movement. *Journal of Neuroscience*, *5*, 2318–2330.

Battaglini, P., Muzur, A., Galleti, C., Skrap, M., & Fattori, A. (2002). Effects of lesions to area v6a in monkeys. *Experimental Brain Research*, *144*(3), 419–422.

Bootsma, R., Marteniuk, R., MacKenzie, C., & Zaal, F. (1994). The speed-accuracy trade-off in manual prehension: effects of movement amplitude, object size and object width on kinematic characteristics. *Experimental Brain Research*, *98*, 535–541.

Bullock, D., Bongers, R., Lankhorst, M., & Beek, P. (1999). A vector-integration-to-endpoint model for performance of viapoint movements. *Neural Networks*, *12*, 1–29.

Bullock, D., Cisek, P., & Grossberg, S. (1998). Cortical networks for control of voluntary arm movements under variable force conditions. *Cerebral Cortex*, *8*(1), 1–15.

Bullock, D., & Grossberg, S. (1988a). Neural dynamics of planned arm movements: emergent invariants and speed-accuracy properties during trajectory formation. *Psychological Review*, *95*(1), 49–90.

Bullock, D., & Grossberg, S. (1988b). The VITE model: a neural command circuit for generating arm and articulator trajectories. In J. Kelso, A. Mandell, & M. Shlesinger (Eds.), *Dynamic patterns in complex systems* (pp. 206–305). Singapore: World Scientific.

Bullock, D., & Grossberg, S. (1991). Adaptive neural networks for control of movement trajectories invariant under speed and force rescaling. *Human Movement Science*, *10*, 3–53.

Castiello, U., Stelmach, G., & Lieberman, A. (1993). Temporal dissociation of the prehension pattern in Parkinson's disease. *Neuropsychologia*, *31*(4), 395–402.

Cisek, P., Grossberg, S., & Bullock, D. (1998). A cortico-spinal model of reaching and proprioception under multiple task constraints. *Journal of Cognitive Neuroscience*, *10*, 425–444.

Contreras-Vidal, J., Ulloa-Perez, A., Lopez-Coronado, J., & Calabozo-Moran, J. (2001). Neural dynamics of hand pre-shaping during prehension. In *Proceedings of the 2001 IEEE conference on systems, man, and cybernetics. Vol. 5* (pp. 3019–3024)

Dessing, J., Bullock, D., Peper, C., & Beek, P. (2002). Prospective control of manual interceptive actions: comparative simulations of extant and new model constructs. *Neural Networks*, *15*, 163–179.

Donoghue, J., Leibovic, S., & Sanes, J. (1992). Organization of the forelimb area in squirrel monkey motor cortex: representation of digit, wrist, and elbow muscles. *Experimental Brain Research*, *89*, 1–19.

Ehrsson, H., Fagergren, A., Jonsson, T., Westling, G., Johansson, R., & Forssberg, H. (2000). Cortical activity in precision-versus power-grip tasks: an FMRI study. *Journal of Neurophysiology*, *83*(1), 528–536.

Feldman, A. (1986). Once more on the equilibrium-point hypothesis (lambda model) for motor control. *Journal of Motor Behavior*, *18*, 17–54.

Fitts, P. (1954). The information capacity of the human motor system in controlling the amplitude of movement. *Journal of Experimental Psychology*, *47*, 381–391.

Fogassi, L., Gallese, V., Buccino, G., Craighero, L., Fadiga, L., & Rizzolati, G. (2001). Cortical mechanism for the visual guidance of hand grasping movements in the monkey: a reversible inactivation study. *Brain*, *124*(Part 3), 571–586.

Gallese, V., Murata, A., Kaseda, M., Niki, N., & Sakata, H. (1994). Deficit of hand preshaping after muscimol injection in monkey parietal cortex. *Neuroreport*, *5*(12), 1525–1529.

Haggard, P., & Wing, A. (1995). Coordinated responses following mechanical perturbation of the arm during prehension. *Experimental Brain Research*, *102*, 483–494.

Hoff, B., & Arbib, M. (1993). Models of trajectory formation and temporal interaction of reach and grasp. *Journal of Motor Behavior*, *25*(3), 175–192.

Hofsten, C. v., & Ronnqvist, L. (1988). Preparation for grasping an object: a developmental study. *Journal of Experimental Psychology: Human Perception and Performance*, *14*(4), 610–621.

Jakobson, L., & Goodale, M. (1991). Factors affecting higher-order movement planning: a kinematic analysis of human prehension. *Experimental Brain Research*, *86*, 199–208.

Jeannerod, M. (1984). The timing of natural prehension movements. *Journal of Motor Behavior*, *16*(3), 235–245.

Jeannerod, M. (1999). Visuomotor channels: their integration in goal directed actions. *Human Movement Science*, *18*, 201–218.

Jeannerod, M., Arbib, M., Rizzolatti, G., & Sakata, H. (1995). Grasping objects: the cortical mechanisms of visuomotor transformation. *Trends in Neurosciences*, *18*(7), 314–320.

Jeannerod, M., Decety, J., & Michel, F. (1994). Impairment of grasping movements following a bilateral posterior parietal lesion. *Neuropsychologia*, *32*(4), 369–380.

Lemon, R., & Mantel, G. (1989). The influence of changes in discharge frequency of corticospinal neurons on hand muscles in the monkey. *Journal of Physiology*, *413*, 315–378.

Lemon, R., Mantel, G., & Muir, R. (1986). Corticospinal facilitation of hand muscles during voluntary movement in the conscious monkey. *Journal of Physiology*, *381*, 497–527.

Middleton, F., & Strick, P. (2000). Basal ganglia and cerebellar loops: motor and cognitive circuits. *Brain Research Reviews*, *31*(2/3), 236–250.

Mon-Williams, M., & Tresilian, J. (2001). A simple rule of thumb for elegant prehension. *Current Biology*, *11*, 1058–1061.

Morasso, P. (1981). Spatial control of arm movements. *Experimental Brain Research*, *42*, 223–227.

Mountcastle, V., Lynch, J., Georgopoulos, A., Sakata, H., & Acuna, C. (1975). Posterior parietal association cortex of the monkey: command functions for operations within extrapersonal space. *Journal of Neurophysiology*, *38*, 871–908.

Nagasaki, H. (1989). Asymmetric velocity and acceleration profiles of human arm movements. *Experimental Brain Research*, *74*, 319–326.

Paulignan, Y., & Jeannerod, M. (1996). Prehension movements. The visuomotor channels hypothesis revisited. In A. Wing, P. Haggard, & J. Flanagan (Eds.), *Hand and brain: the neurophysiology and psychology of hand movements, Chap. 13* (pp. 265–282). London: Academic Press.

Paulignan, Y., Jeannerod, M., MacKenzie, C., & Marteniuk, R. (1991a). Selective perturbation of visual input during prehension movements. Part 2. The effects of changing object size. *Experimental Brain Research*, *87*, 407–420.

Paulignan, Y., MacKenzie, C., Marteniuk, R., & Jeannerod, M. (1991b). Selective perturbation of visual input during prehension movements. Part 1. The effects of changing object position. *Experimental Brain Research*, *83*, 502–512.

Peper, L., Bootsma, R., Mestre, D., & Bakker, F. (1994). Catching balls: how to get the hand to the right place at the right time. *Journal of Experimental Psychology: Human Perception and Performance*, *20*(3), 591–612.

Roy, A., Paulignan, Y., Farne, A., Jouffrais, C., & Boussaoud, D. (2000). Hand kinematics during reaching and grasping in the macaque monkey. *Behavioural Brain Research*, *117*, 75–82.

Saling, M., Mescheriakov, S., Molokanova, E., Stelmach, G., & Berger, M. (1996). Grip reorganization during wrist transport: the influence of an altered aperture. *Experimental Brain Research*, *108*, 493–500.

Schwartz, A. (1994). Neuronal substrate for volitional movement. In K. Bennet, & U. Castiello (Eds.), *Insights into the reach to grasp movement* (*Vol. 105*) (pp. 59–83). *Advances in psychology, Chap. 4. Central mechanisms*. Amsterdam: Elsevier.

Taira, M., Mine, S., Georgopoulos, A., Murata, A., & Sakata, H. (1990). Parietal cortex neurons of the monkey related to the visual guidance of hand movement. *Experimental Brain Research*, *83*, 29–36.

Tanji, J., Kazuhiko, O., & Sato, K. (1988). Neuronal activity in cortical motor areas related to ipsilateral, contralateral and bilateral digit movements of the monkey. *Journal of Neurophysiology*, *60*(1), 325–343.

Tannee, J., Boussaoud, D., Boyer-Zeller, N., & Rouiller, E. (1995). Direct visual pathways for reaching movements in the macaque monkey. *NeuroReport*, *7*(1), 267–272.

Timmann, D., Stelmach, G., & Bloedel, J. (1996). Grasping component alterations and limb transport. *Experimental Brain Research*, *108*, 486–492.

Ulloa, A., Bullock, D., & Rhodes, B. (2003). Adaptive force generation for precision-grip lifting by a spectral timing model of the cerebellum. *Neural Networks* [doi: 10.1016/S0893-6080(03)00094–7].

Wallace, S., & Weeks, D. (1988). Temporal constraints in the control of prehensile movement. *Journal of Motor Behavior*, *20*(2), 81–105.

Wenger, K., Musch, K., & Mink, J. (1999). Impaired reaching and grasping after focal inactivation of globus pallidus pars interna in the monkey. *Journal of Neurophysiology*, *82*, 2049–2060.

Wing, A., Turton, A., & Fraser, C. (1986). Grasp size and accuracy of approach in reaching. *Journal of Motor Behavior*, *18*(3), 245–260.

Zaal, F., Bootsma, R., & van Wieringen, P. (1998). Coordination in prehension. Information-based coupling of reaching and grasping. *Experimental Brain Research*, *119*, 427–435.

Zhang, X., & Chaffin, D. (1999). The effects of speed variation of joint kinematics during multi-segment reaching movements. *Human Movement Science*, *18*, 741–757.